U. S. DEPARTMENT OF COMMERCE
NATIONAL OCEANIC AND ATMOSPHERIC ADMINISTRATION
NATIONAL WEATHER SERVICE
NATIONAL METEOROLOGICAL CENTER

OFFICE NOTE 371

An Operational Marine Fog Prediction Model

JORDAN C. ALPERT[†]

DAVID M. FEIT*

JUNE 1990

THIS IS AN UNREVIEWED MANUSCRIPT, PRIMARILY INTENDED FOR INFORMAL EXCHANGE OF INFORMATION AMONG NWS STAFF MEMBERS

[†] Global Weather and Climate Modeling Branch

* Ocean Products Center

OPC contribution No. 45

An Operational Marine Fog Prediction Model

Jordan C. Alpert and David M. Feit

NOAA/NMC, Development Division

Washington D.C. 20233

Abstract

A major concern to the National Weather Service marine operations is the problem of forecasting advection fogs at sea. Currently fog forecasts are issued using statistical methods only over the open ocean domain but no such system is available for coastal and offshore areas. We propose to use a partially diagnostic model, designed specifically for this problem, which relies on output fields from the global operational Medium Range Forecast (MRF) model. The boundary and initial conditions of moisture and temperature, as well as the MRF's horizontal wind predictions are interpolated to the fog model grid over an arbitrarily selected coastal and offshore ocean region. The moisture fields are used to prescribe a droplet size distribution and compute liquid water content, neither of which is accounted for in the global model. Fog development is governed by the droplet size distribution and advection and exchange of heat and moisture. A simple parameterization is used to describe the coefficients of evaporation and sensible heat exchange at the surface. Depletion of the fog is based on droplet fallout of the three categories of assumed droplet size.

Comparison of three months of model results over the Atlantic seaboard with ship data show realistic forecasts of fogbound areas. The MRF initial conditions are used to update the fog model boundaries, thus supplying "perfect forecasts" for the fog model

boundary conditions. Liquid water droplet concentrations are used to infer the relative intensity of fog and compare well with visibility reports from ship locations. It should be noted, however, that the verification of fog at sea is hampered by the limited amount of routinely available ship observations. The model also successfully predicted situations in which no fog was present when similarly verified with ship data. These results show that diagnostic models can be developed for specific regional applications based on numerical weather forecasts made with large scale global models.

Introduction

Advection fogs at sea are a persistent problem of major concern to the marine meteorologist. Fog formed in this manner seriously hampers navigation and is hazardous to marine transportation. Some of the results from numerical simulations of marine advection fogs by Feit (1972) and Barker (1973), suggest that one can successfully develop a predictive technique for maritime fog in an operational setting. The operational aspect imposes a number of technical problems and requirements on a marine fog model. These include ensuring timely forecasts, consistent accuracy, and obtaining initial and boundary conditions from ocean regions that may contain few observations.

Forecasting mesoscale fog formation and dissipation has been attempted in two basic ways: (1) through an empirical approach using data; and (2) through a theoretical approach based on the physical processes involved. An example of the former approach is the study by Taylor (1917). Taylor produced what is still the most definitive case study of advection fog along the Grand Banks. More recently Burroughs (1989) developed a statistical method of predicting fog over the open oceans of the northern hemisphere oceans. This method is now implemented in the current NMC operational system and produces routine fog forecasts during the warm season (Apr–Oct). Pettersen (1939), Swinbank (1945) and George (1960) also sought out empirical relations while the work of Rodhe (1962), Fisher and Caplan (1963) and Barker (1973) are representative of the second approach. The latter is an example of a dynamical fog model for use over ocean areas. However, the model described in the present paper is the first dynamical model routinely used in an operational setting.

Advective fogs are formed when the trajectory of the air brings it from a warmer underlying surface to a colder underlying surface. For this reason it is primarily a spring–summer phenomenon which occurs most commonly in and near coastal regions. Some preferred areas are the Grand Banks region in the Atlantic and the waters near Japan.

Model Description

To simulate the formation of fog and stratus, time dependent changes of temperature, water vapor and liquid water content are predicted. The changes in the atmospheric variables of temperature, water vapor and liquid water content are described by the following equations:

$$\frac{\partial \Theta}{\partial t} = K_h \nabla_h^2 \Theta + \frac{\partial}{\partial z}\left(K_z \frac{\partial \Theta}{\partial z}\right) - \vec{\mathbf{V}}_3 \cdot \nabla \Theta + S_H$$

$$\frac{\partial q}{\partial t} = K_h \nabla_h^2 q + \frac{\partial}{\partial z}\left(K_z \frac{\partial q}{\partial z}\right) - \vec{\mathbf{V}}_3 \cdot \nabla q + S_q$$

$$\frac{\partial w}{\partial t} = K_h \nabla_h^2 w + \frac{\partial}{\partial z}\left(K_z \frac{\partial w}{\partial z}\right) - \vec{\mathbf{V}}_3 \cdot \nabla w + S_w$$

where Θ, is the potential temperature, q, is mixing ratio and w, is liquid water and S_H, S_q, and S_w are the sources or sinks of heat, water vapor or liquid water respectively. The K's in the interior of the model are computed using K–theory eddy diffusion and described in the following section. The above system is solved by standard finite difference techniques.

Horizontal velocity fields for the forecast period are obtained from NMC's MRF model (Sela, 1980 and 1982). These velocities are used to advect heat, moisture and liquid water. The lateral boundary conditions and initial conditions for the fog model are supplied by the MRF model operational forecast fields. The MRF model is global spectral with triangular 80 truncation (NMC Development Division, Staff document, 1988).

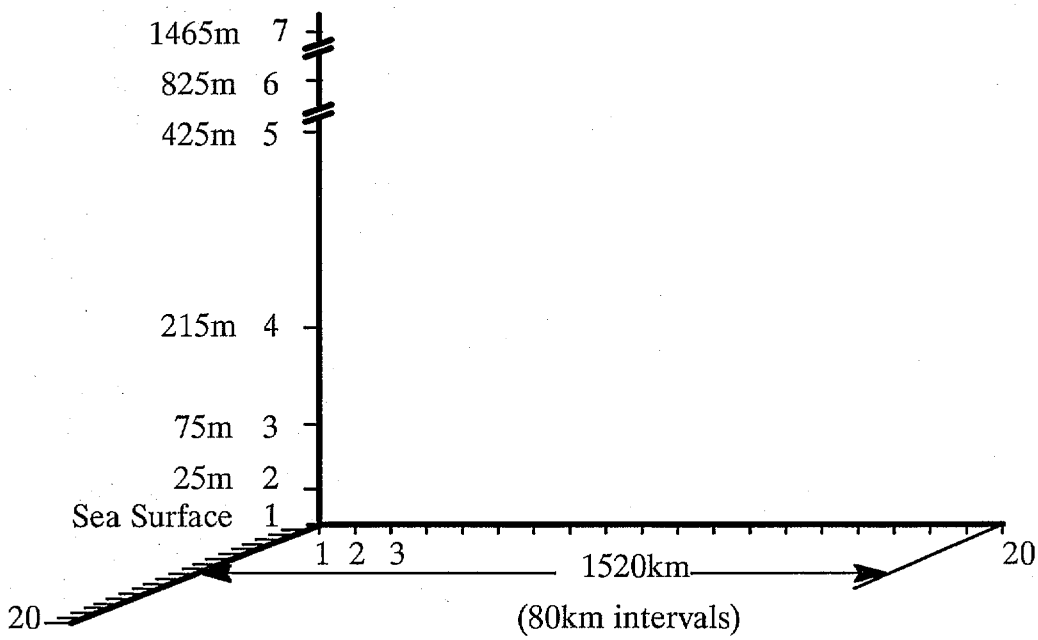

Fig. 1 Fog model grid dimensions.

Experiments were carried out to find a favorable vertical and horizontal model resolution fog model. The result was a 20 by 20 point horizontal grid, 1520 km extent, 7 vertical layers, lowest model level at 25 meters above the sea surface, and top of the model close to 2 km. A diagram of the vertical and horizontal structure of the fog model domain is shown in Fig. 1. The vertical levels have been designed to approximately coincide with the first 5 MRF model sigma levels starting with the fog model level 3. The fog model level 2, at 25m, is the level used to determine the fog conditions. Experiments at a higher vertical resolution, a 20 layer model, with the lowest layer at 10 m, showed only minor differences compared to the 7 layer model.

Boundary and Initial Conditions

The importance of the initial conditions can not be overestimated in fog prediction. The use of many different sources of data including satellite, aircraft, buoys, and ships is needed for this purpose. Initial conditions for the global MRF model are provided by the Global Data Assimilation System (GDAS). The GDAS (Dye and Morone, 1985) uses available observations and first guess MRF model fields to perform an optimal interpolation analysis on every 6–hour synoptic cycle. These fields contain past information due to the cycling of the simulation system so a certain amount of observed information can be advected from data rich areas to adjacent data sparse areas. The initial conditions for the fog model are obtained from the GDAS analysis. Forecast fields of winds (u, v) over the entire domain and boundary values for temperature, moisture and surface pressure (Θ, q, and P_S) are then obtained from the MRF. The MRF does not carry liquid water content as a dependent variable or droplet size distribution which are necessary for modeling fog. Thus, an essential feature of a fog model is the inclusion of detailed moist physics, to a degree greater than is presently considered in the operational MRF.

The boundary conditions, Θ, q, u, v, and surface pressure, P_S, are normally obtained from the MRF model and drawn from NMC operational forecast sigma level files. However, since these forecasts are not archived, the integrations following used MRF initial condition fields instead of forecasts. A sponge layer is used on lateral boundaries to facilitate a smooth transition from the large scale model to the fog model. Boundary values are updated by the fog model advective scheme only if there is advection from the fog model interior domain to the boundaries. Otherwise, the lateral boundaries are interpolated linearly in time from MRF 12 hour forecasts. The lower boundary temperature is prescribed by the Ocean Products Center blended analysis of sea surface temperature. This is held constant for the duration of the fog model run. The MRF vertical sigma coordinate is interpolated to the fog model's z coordinate. Since the horizontal resolution of the fog model is about double that of the MRF global spectral model, horizontal interpolation is used to transform the MRF's gaussian grids to the fog model's domain. Vertical motion is diagnosed from continuity.

First Layer Flux Calculations and Interior Diffusion

Physical processes included in the fog model are eddy diffusion, horizontal advection, and fog droplet fallout. Fluxes of heat and water vapor are calculated starting with the following simple system of equations applied at layer 1:

$$F_{H_1} = -\varrho c_p C_H \left(\frac{\partial \Theta}{\partial z} \right)_1 \qquad F_{E_1} = -\varrho C_E \left(\frac{\partial q}{\partial z} \right)_1 ,$$

where: F_{H1} and F_{E1} are the flux of heat and water vapor respectively between the ocean and the first model layer, ρ is the air density, c_p is the heat capacity at constant pressure, and C_H and C_E are the exchange coefficient of sensible heat and moisture respectively. This formulation is further simplified by setting the constant for the exchange coefficients of sensible heat and evaporation/condensation equal, viz., $C_H = C_E =$ constant. Tests have been made of other parameterization formulations including Richardson number dependent formulations (Deardorff, 1968). However, the results from these experiments did not change the fog predictions substantially through 36 hours, thus, we use the simplest formulation.

The fog model diffusion is handled by calculating exchange coefficients, K_z, at interior model levels z for Θ, q, and w as in Blackadar (1962):

Ri < (Ri)$_{crit}$ $$K_z = l^2 \left| \frac{d\vec{V}}{dz} \right| (1 - 18R_i)$$

Ri > (Ri)$_{crit}$ $$K_z = l^2 \frac{\left| \frac{d\vec{V}}{dz} \right|}{(1 + 18R_i)}$$

where $$l = \frac{0.4z}{1 + 0.00027z \left| \frac{U_{top}}{f} \right|}$$

and where (Ri)$_{crit}$ is 0.25 and U_{top} is the wind speed at the top level.

Moist Processes and Fog Forecasts

The system is adjusted by a wet bulb process to a quasi– equilibrium relative humidity of 99%. This equilibrium is achieved in the following way. If the ambient conditions indicate super saturation (relative humidity > 99%) one half of the excess vapor is condensed and the appropriate change to liquid water content and temperature is made. The equilibrium relative humidity is approximated by condensing either one half of the excess water vapor or evaporating one half of the liquid water content. The potential temperature is then changed by using a wet bulb adjustment as shown in Fig 2. The amount of under/over saturation, called the vapor residual value (excess or deficiency), is computed from $E - E_s$, where E is the water vapor pressure and E_s is the saturation vapor pressure. If the under/over saturation is greater than a critical value, then the thermodynamic calculations proceed.

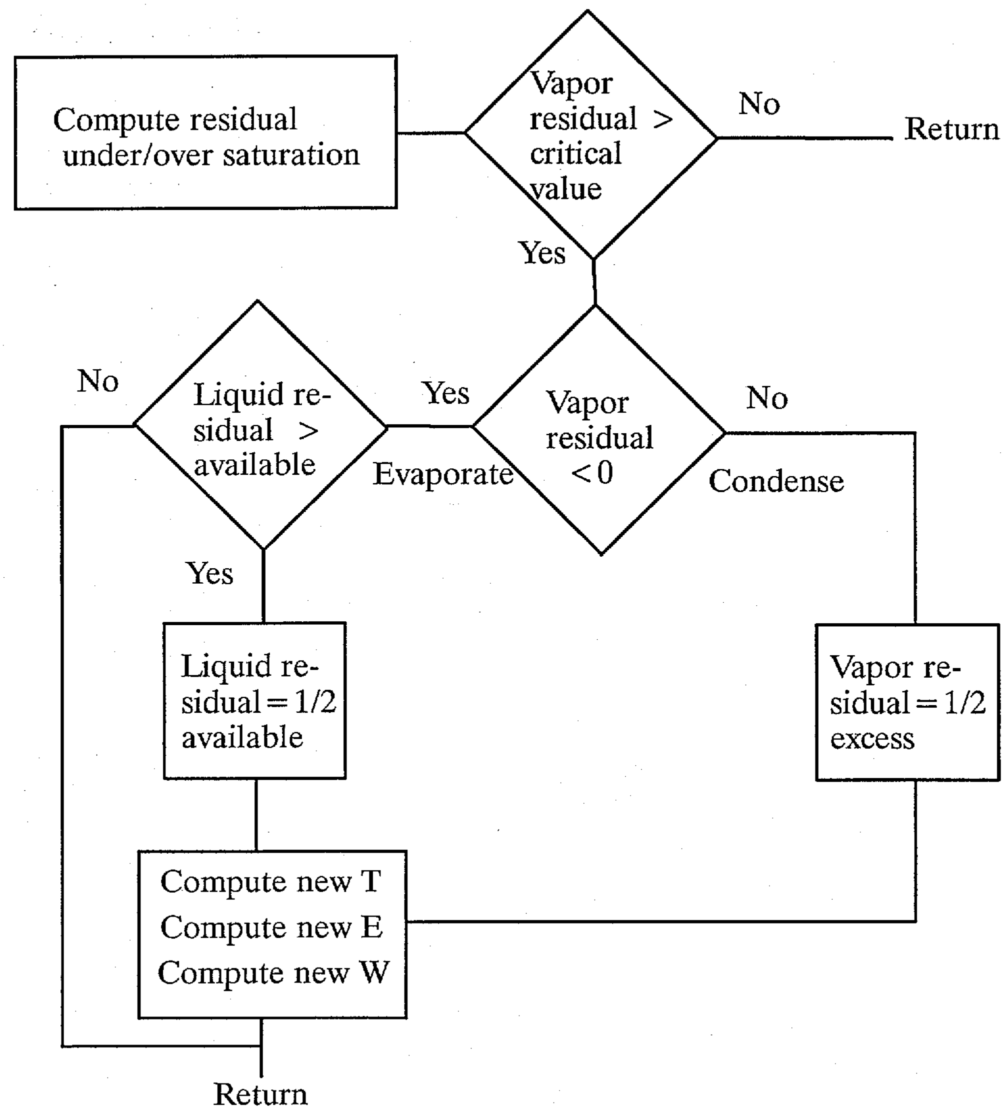

Fig. 2 Schematic fog model moist physics.

If the vapor residual is less than zero evaporation takes place. A "liquid residual" is then computed by converting one–half of this vapor residual into an equivalent amount of liquid which is subtracted from the reservoir of available liquid. A new temperature is calculated based on the amount of heat from the evaporation of water.

If the vapor residual is greater than zero then condensation takes place. A new temperature is calculated based on the amount of heat from the condensation of water. At the same time new water vapor and liquid water is computed as a result of the new temperature. This means that at the end of the process shown in Fig 2, there is an imbalance between the temperature, water vapor and liquid water. The imbalance is allowed to persist until the next model time step where new state variables are computed and the processes shown in Fig 2 are repeated.

A simple parameterization of droplet fallout is used which contains three categories of droplet sizes as follows:

% Number by Mass	Droplet Radius	Terminal velocity
25	5μ	0.39 cm s^{-1}
50	20μ	4.75 cm s^{-1}
25	30μ	10.75 cm s^{-1}

The terminal velocities combined with the droplet sizes permits the flux of liquid water loss to be calculated.

The main output of the fog model is a liquid water content prediction. The relationship between liquid water content and visibility has been studied by Wiener *et. al.* (1961). Using the results of this study, Fig 3, a binary prediction of fog or no fog is made by assigning a critical value for liquid water of 0.04 grams/m^3. This corresponds to a visibility of 1–2000 ft.

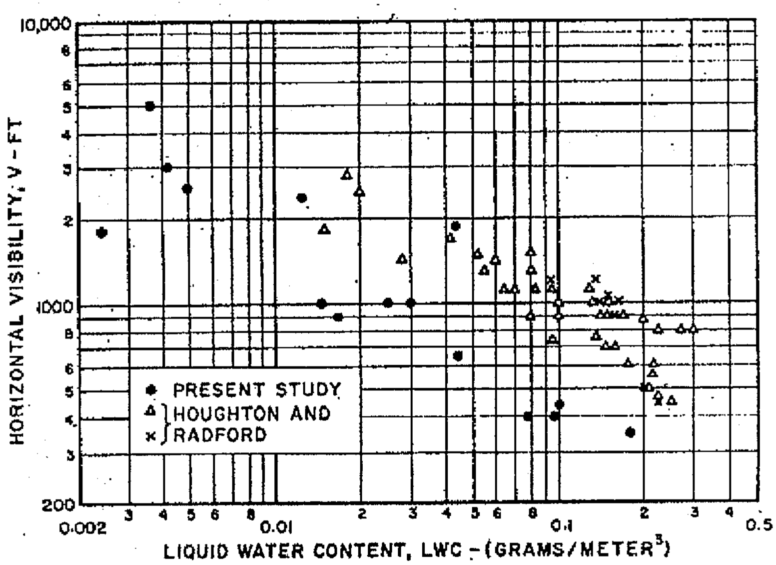

Fig. 3 Horizontal visibility in ocean fog as a function of liquid water content (after Wiener *et. al*. 1961).

Fog Model Verification

For objective verification, actual ship observations were compared to model run data. The model run data was collected for three months (June, July, and August) in 1989. A total of 87 forecast days were integrated each extending to 36 hours. MRF model history fields, including liquid water content for 12, 24 and 36 hour forecast, were saved and interpolated to a form comparable with the ship observation data set. Verifying initial conditions were used to update the model boundaries at 12 hour intervals. This means that the fields used to update the fog model boundaries during the integration of these experiments are from "perfect forecasts" of the MRF model, therefore, the results of these experiments are a measure of the upper limits of the fog model's capabilities.

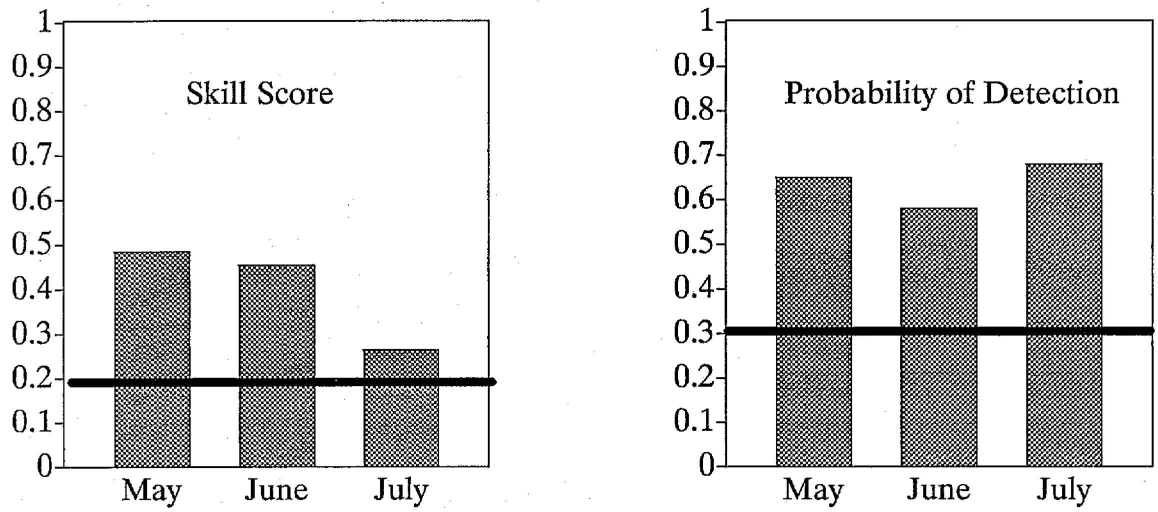

Fig. 4 Skill score (left) and the probability of detection (right) for a 36 hour fog model forecast verified against ship data. The solid line is the average score for spring from the operational statistical forecast.

The verification of the model liquid water content predictions presents certain problems. The observed present weather recorded from ship observations only has the opportunity to report one type of present weather event though several may be occurring simultaneously. For example, if rain and fog are occurring together, a not uncommon phenomena, only rain would be reported. Therefore, an upper bound was established on the predictions of liquid water content such that fog was not predicted at locations at which it was raining. The value of 0.8 grams/m^3 was used for the upper bound of fog liquid water. Values greater than this amount were considered, for verification purposes, rain.

Figure 4 shows the normalized Gringorten skill score (Burroughs, personal communication, 1990) and probability of detection for 36 hour model forecasts verified against ship data. The skill score used is referenced against climatology so that zero indicates no skill while perfect forecasts have a skill of 1. The solid line shown in Figs 4 and 5 are the 3 month average scores from the operational statistical fog model. Since these scores apply to the entire North Atlantic ocean and were made with operational model output, not with "perfect forecasts", they are used only as a general reference. Some tests were made verifying the operational statistical system in the area used for the fog model forecasts. These scores (not shown) were even lower in that area than the solid lines indicate. This is not surprising because the statistical system is not well suited to coastal and off shore areas. The probability of detection is shown in Fig 4 (right). This indicates the number of correct forecasts of fog divided be the number of fog observations. A perfect score is 1. Current operations, as mentioned above, display a range of from 0.3 – 0.5 for the probability of detection.

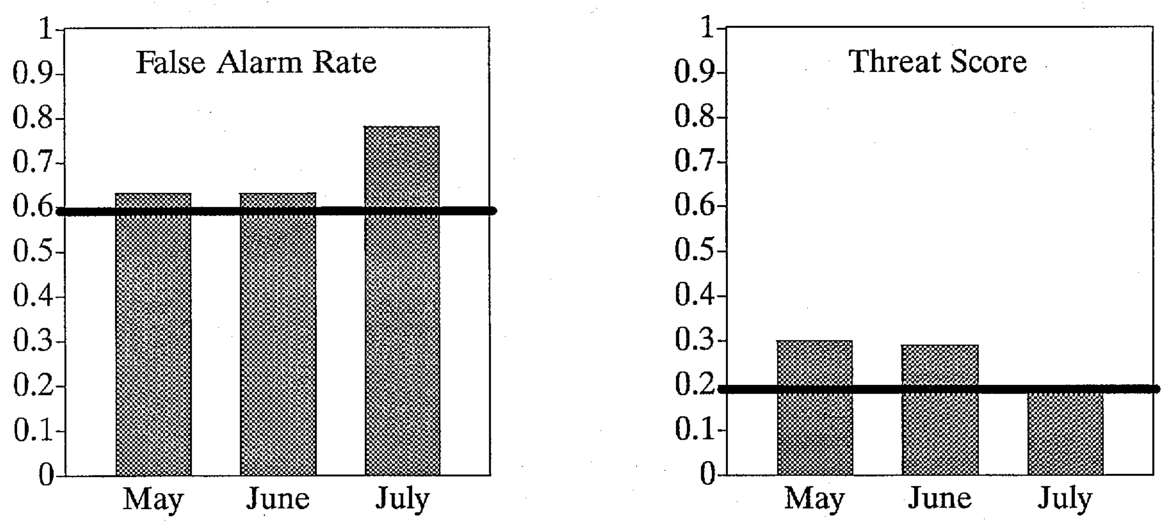

Fig. 5 False alarm rate (left) and the threat score (right) for a 36 hour fog model forecast verified against ship data. The solid line is the average score for spring from the operational statistical forecast.

Figure 5 shows the false alarm rate and the threat score for the same forecasts as in Fig. 4. The false alarm rate is the number of times fog was forecast and did not occur divided by the number of times fog was forecast. A perfect score for false alarm rate is zero. Although these scores may be considered high it should be noted that these statistics are based on individual ship reports which may or may not reflect the areal extent of fog. The Threat score is the number of correct forecasts (fog and no fog) divided by the total number of forecasts made with the number of no fog forecasts subtracted from the numerator and denominator. A perfect score would be 1.

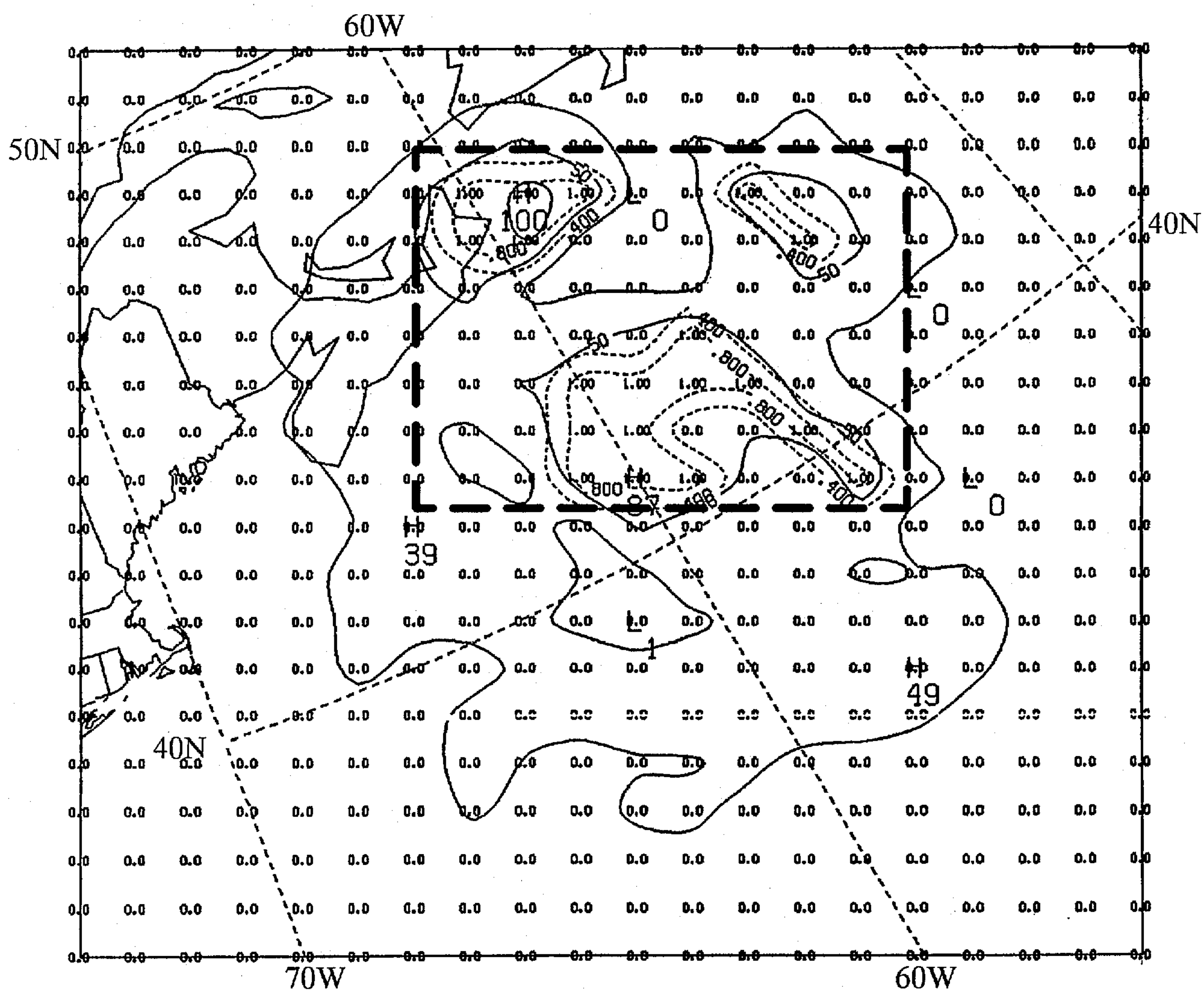

Fig. 6 36hr Fog model prediction valid 12z, 10 May 89. The dashed box represents the approximate fog bound area forecast by the model.

The deterioration of scores in July may be attributed to the fact that there was little occurrence of fog in the model domain and many rain events which may have masked coincident fog events. A subjective evaluation of observations on individual days in July, including ship observations compared with model forecasts from surface synoptic charts (not shown), indicate that the fog model performance was similar to previous months. We suspect that the verification of fog occurrence was preempted by the requirement of vessels to report rain over fog.

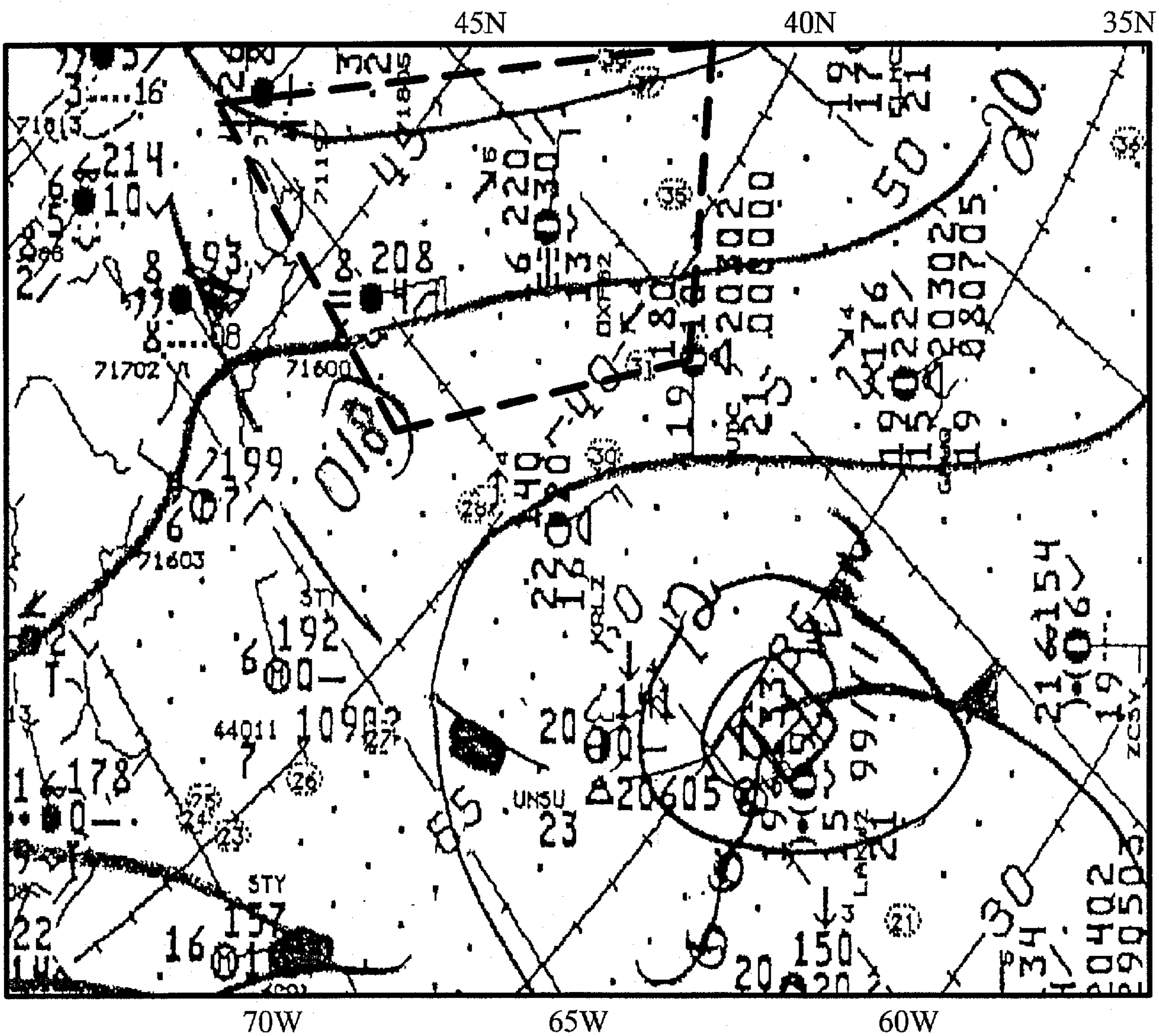

Fig. 7 Surface Synoptic chart for 12z, 10 May 89. The dashed box represents the approximate fog bound area forecast by the model as shown in Fig. 6

A typical 36 hour fog forecast is shown in Fig 6 valid 12z, 10 May 8. The solid contours in Fig 6 measure liquid water content every 0.04 gm/m^3. The dash contours represent the areas where liquid water amounts exceeded 0.04 gm/m^3 and the assignment of a 1.0 or 0.0

to each model grid point on Fig 6, indicates a binary representation of fog and no fog respectively. The dashed box represents the approximate fog bound area forecast by the model. The verifying surface analysis is shown in Fig 7 including the re–mapped dashed box from Fig 6. The map projections differ, thus distorting the shape of the bounded area. The forecast fog bound area is shown to be in the vicinity of ships reporting fog and, when examined subjectively, would be considered useful by the marine forecaster. The individual ship reports, however, appear outside the fog model's fog bound regions, thus this forecast would score low on the skill measures shown in Figs. 4 and 5.

Conclusion

In this study we have presented a relatively simple, partially diagnostic, boundary layer model designed specifically for forecasting marine advection fog. It uses MRF forecast fields as input and may be viewed as a value added adjunct. The model takes about a minute to run on the NMC Cray computer and accounts for fields not considered in detail in the NMC global or regional models, viz., boundary layer liquid water content. An evaluation of model forecasts over a 87 day period show that it is possible to produce useful objective forecasts of marine advection fog when the MRF model makes a good forecast. MRF model global predictions correlate better than .9 with verification at 48 hour forecasts so it is expected that the fog model forecasts will not degrade significantly when MRF forecasts are used to update the boundaries. It is also expected that improved model forecasts will result from the inclusion of radiation physics and a more complex fog droplet fallout scheme for water droplet depletion.

Acknowledgments

The authors wish to acknowledge L. Burroughs for his valuable contribution to the verification of the fog model forecasts and D. B. Rao for stimulating discussions and helpful suggestions. We also thank V. Gerald for supplying the archive tape of ship data.

References

Barker, E. H., 1973; Oceanic fog, a Numerical Study., *ENVPREDRSCHFAC Tech. paper No. 6–73*, Naval Postgraduate School, Monterey, CA 65pp.

Blackadar, A. K., 1962 : The vertical distribution of wind and turbulent exchange in a neutral atmosphere. *J. of Geoophy. Res.*, **67** (8), pp. 3095–3102

Burroughs, L. D., 1989: Forecasting open ocean fog and visibility. *Proceedings 11th Conference on Probability and Statistics*, October 1–5, Monterey, CA, pp 45–49.

Dye C. H., and L. L. Morone, 1985: Evolution of the National Meteorological Center Global Data Assimilation System: January 1982, December 1983., *Mon. Wea. Rev* , 113, pp 304–318.

Feit, D. M., 1972: A study of numerical simulation of maritime fog., *ENVPREDRSCHFAC Tech. Paper, No. 13–72*, Naval Postgraduate School, Monterey, CA, 46pp.

Fisher, E. L. and P. Caplan, 1963: An experiment in numerical predictions of fog and stratus., *J of Atmos. Sci*, **20**, pp 425–437

Gandin, L. S., 1963: *Objective Analysis of Meteorological Fields*, Gidrometeorologicheskoe Izdatel'stvo, Leningrad. Translated from Rusian, Isreal Program for Scientific Translations, 1965, 242pp.

George, J. J., 1960: *Weather forecasting for aeronautics.*, New York, Academic Press.

NMC Development Division, Staff document, 1988: *Documentation of the research version of the NMC Medium Range Forecatsting model.*, 350pp.

Pettersen, S., 1939: Some aspects of formation and dissipation of fog., *Geof. Publ. Norw. Acc. of Sci.*, **12**, no. 10.

Rodhe, B., 1962: The effect of turbulence on fog formation. *Tellus*, **XIV**, pp 49–86.

Sela, J. G., 1982: The NMC Spectral Model., NOAA *Technical Report NWS 30,* National Meteorological Center, Washington, D.C. 20233.

Sela, J. G., 1980: Spectral Modeling at the National Meteorological Center., *Mon. Wea. Rev,* **108,** 1279–1292.

Swinbank, W.C., 1945: *Prof. Notes No. 100.*, Met Office, London.

Taylor G.I., 1917: The formation of fog and mist. *Quart. J. Roy. Meteor. Soc.,* 43, pp 241–268.

Wiener, F. M., J. H. Ball, and C. M. Gogos, 1961:, Some micrometeorological measurements in ocean fog., *J. Geo. Res,* **66**, 11, pp 3974–3978.